SCD inhibition eradicates AML displaying high *de novo* fatty acid desaturation and synergizes with chemotherapy

Vilma Dembitz[1,2], Hannah Lawson[1], Richard Burt[3,4], Céline Philippe[1], Sophie C. James[1], Samantha Atkinson[3,4], Jozef Durko[1], Lydia M. Wang[1], Joana Campos[1], Aoife M. S. Magee[1], Keith Woodley[1], Michael Austin[1], Ana Rio-Machin[5], Pedro Casado-Izquierdo[5], Findlay Bewicke-Copley[5], Giovanny Rodriguez Blanco[6], Diego Pereira Martins[7], Lieve Oudejans[7], Emeline Boet[8,9], Alex von Kriegsheim[6], Juerg Schwaller[10], Andrew J. Finch[11], Bela Patel[1], Jean-Emmanuel Sarry[8,9], Jerome Tamburini[12], Jan Jacob Schuringa[7], Lori Hazlehurst[13], John A. Copland, III[14], Mariia Yuneva[4], Barrie Peck[11], Pedro Cutillas[5], Jude Fitzgibbon[5], Kevin Rouault-Pierre[1], Kamil Kranc[1] and Paolo Gallipoli[1]*

[1] Centre for Haemato-Oncology, Barts Cancer Institute, Queen Mary University of London, London EC1M 5PZ, UK, [2] Department of Physiology and Croatian Institute for Brain Research, University of Zagreb School of Medicine, 10000 Zagreb, Croatia, [3] Division of Cell and Molecular Biology, Imperial College London, London SW7 2BX, UK, [4] Francis Crick Institute, London NW1 1AT, UK, [5] Centre for Cancer Genomics & Computational Biology, Barts Cancer Institute, Queen Mary University of London, London EC1M, London, UK, [6] The University of Edinburgh MRC Institute of Genetics and Cancer, University of Edinburgh, Edinburgh, EH4 2XU, UK, [7] Department of Experimental Hematology, University Medical Center Groningen, University of Groningen, 9713 GZ, Groningen, The Netherlands., [8] Centre de Recherches en Cancérologie de Toulouse, Université de Toulouse, Inserm U1037, CNRS U5077, LabEx Toucan, Toulouse, France, [9] Équipe labellisée Ligue Nationale Contre le Cancer 2023, Toulouse, France, [10] University Children's Hospital and Department of Biomedicine (DBM), University of Basel, 4031 Basel, Switzerland, [11] Centre for Tumour Biology, Barts Cancer Institute, Queen Mary University of London, London EC1M, London, UK, [12] Translational Research Centre in Onco-hematology, Faculty of Medicine, University of Geneva, and Swiss Cancer Center Leman, 1205 Geneva, Switzerland, [13] Modulation Therapeutics, Morgantown, West Virginia 26506, USA, [14] Department of Cancer Biology, Mayo Clinic, Jacksonville, Florida 32224, USA

*Correspondence: Paolo Gallipoli, Centre for Haemato-Oncology, Barts Cancer Institute, Queen Mary University of London, Charterhouse Square, London EC1M 5PZ, UK; e-mail: p.gallipoli@qmul.ac.uk

Running head: SCD inhibition has anti-leukemic effects in AML

Text word count: 4827

Abstract word count: 150

Number of figures: 7

Number of references: 62

KEY POINTS:

- SCD expression is highly prognostic in AML and SCD inhibition is toxic in AML cells displaying high rates of fatty acid desaturation.
- SCD inhibition in combination with conventional chemotherapy prolongs survival in murine AML models.

Abstract:

Identification of specific and therapeutically actionable vulnerabilities in acute myeloid leukaemia (AML) is needed to improve patients' outcome. These features should be ideally present in many patients independently of mutational background. Here we identify *de novo* fatty acid (FA) desaturation, specifically stearoyl-CoA desaturase (SCD) inhibition, as a therapeutic vulnerability across multiple AML models *in vitro* and *in vivo*. SCD inhibition induces AML cell death *via* pleiotropic effects, and sensitivity is based on their dependency on FA desaturation regardless of mutational profile. Its efficacy is enhanced by driving FA biosynthesis *in vitro* and is less prominent *in vivo* due to stromal protection. SCD inhibition increases DNA damage and its combination with standard DNA damage-inducing chemotherapy prolongs survival in aggressive murine AML models. Our work supports developing FA desaturase inhibitors in AML while stressing the importance of identifying predictive biomarkers of response and biologically validated combination therapies to realize their therapeutic potential.

Keywords: AML, SCD, lipotoxicity**,** fatty acid biosynthesis**,** chemoresistance

INTRODUCTION

AML is a highly aggressive malignant clonal disease of hematopoietic origin. Despite the approval of several novel therapies in the past decade, AML prognosis remains poor with long-term survival rates of about 30%[1]. Development of novel therapeutic approaches for AML is particularly challenging due to high genetic and cellular heterogeneity[2], but also because most driver mutations are loss-of-function or transcription factor mutations, and thus difficult pharmacological targets[3]. Therefore, identification of specific AML biological features beyond genetic mutations is needed for development of targeted therapies to improve patient outcomes. Rewired metabolism is one such feature[4], however discerning specific metabolic dependencies of malignant cells is crucial to avoid generalized toxicity that often compromises clinical use of metabolic inhibitors[5].

Fatty acid (FA) metabolism has emerged as a cancer-specific vulnerability in multiple solid cancers[6-9], but its role in haematological malignancies, and specifically AML, is less characterized. Although in AML most preclinical evidence has focused on the role of fatty acid oxidation (FAO) [10-13], targeting FAO is associated with the risk of cardiac toxicity[14] and the best characterised FAO inhibitor, etomoxir, proved to be systemically toxic, halting its clinical development[15]. Comparatively, targeting fatty acid synthesis (FAS), particularly stearoyl-CoA desaturase 1 (SCD1, hereafter SCD), the enzyme converting saturated fatty acids (SFA) palmitate and stearate into monounsaturated fatty acids (MUFA) palmitoleate and oleate[16], appears to be more tolerable based on preclinical studies[17]. SCD plays a role in metabolic adaptation of acute lymphoblastic leukaemia to the central nervous system microenvironment[18] and resistance of AML stem cells to NAMPT inhibitors[19]. Additionally, transcription factor C/AAT-enhancer binding protein α (C/EBPα) regulates lipid biosynthesis in *FLT3*-mutant AML cells by acting on the fatty acid synthase (FASN)-SCD axis, which increases their ability to withstand oxidative stress and leads to greater sensitivity to FLT3 inhibitors upon SCD inhibition[20]. However, the significance of SCD levels in AML prognosis and response to therapy, its functional role, and potential as a therapeutic target, including identification of biological determinants of sensitivity to its inhibition, remain unknown.

Here we address these questions utilising SSI-4, a novel clinical grade SCD inhibitor with a favourable general toxicity profile[21]. We show that SCD expression is prognostic in AML, and its inhibition compromises viability in AML cell lines and primary samples with higher rates of MUFA synthesis, without inducing haematological toxicity in mouse models. SCD activity regulates sensitivity to anthracycline-based treatments and SCD inhibition combined with standard AML chemotherapy prolongs survival in murine models of AML.

METHODS

Cells and cell culture

Primary human AML samples were from Barts Cancer Institute Biobank (n=36) or University Medical Center Groningen (n=11). All human samples were obtained and studied after informed consent and protocol approval by both institutions Ethical Committees and BCI Tissue Biobank's scientific sub-committee in accordance with the Declaration of Helsinki. Details for cell line sources, cells and cell culture are provided in the supplemental methods.

Animal studies

For xenograft models, AML cells were injected into the tail veins of NOD.Cg-*Kit*$^{W-41J}$*Tyr*$^{+}$*Prkdc*^{scid} *Il2rg*^{tm1Wjl}/ThomJ (NBSGW) mice. For murine AML modelling, inducible *MLL-AF9* mouse LSK cells were tail vein injected into CD45.1^{+}/CD45.2^{+} recipient mice together with unfractionated support CD45.1^{+}

wild-type BM cells. Animals were culled either at pre-defined treatment endpoints or, for survival experiments, after reaching humane endpoints. See the supplemental methods for details.

Cell viability

Cell viability was determined using FITC-conjugated anti-Annexin V antibody with propidium iodide or Zombie NIR™ (BioLegend) stains or PE-conjugated anti-Annexin V antibody with 7-AAD stain. Double negative cells were deemed viable. Details of flow cytometric analyses are available in supplemental methods.

Western blotting

The protein extracts were subjected to SDS–PAGE and transferred onto PVDF membranes using wet transfer. Membranes were incubated overnight at 4 °C with primary antibodies and 2h at RT with secondary antibodies. Bands were visualized using an Amersham Imager (GE Healthcare) or a ChemiDoc Imaging system (BioRad).

RNA sequencing and analysis

RNA Sequencing and basic analysis was provided by Novogene UK Company Limited (Cambridge, UK). Complete description is available in supplemental methods.

Metabolomics experiments

For lipidomics analysis, lipid species were extracted from cell pellets using monophasic isopropanol extraction and analysed using liquid chromatography and a Q Exactive™ Hybrid Quadrupole-Orbitrap™ Mass Spectrometer (ThermoFisher). For fatty acid profiling, apolar metabolites were isolated from cells using chloroform:methanol extraction (2:1, v/v, both HPLC grade, Fisher) and fatty acids partitioned from polar metabolites by resuspension of dried extracts in chloroform:methanol:water (1:3:3, v/v, HPLC grade, Fisher). Data acquisition was performed using an Agilent 7890B-7000C GC-triple-quadrupole MS. Details of metabolomics analyses are provided in supplemental methods.

Statistical analysis and reproducibility

Overall survival was plotted using Kaplan–Meier plots, using Cox proportional hazard regression to compare the differences between the curves. The difference between multiple experimental groups was analysed by two-way ANOVA (Kruskal–Wallis test with post hoc Dunn analysis) or two-tailed paired or unpaired Student's t test. IC50 and cell viability curves were determined using non-linear regression analyses. Correlation was calculated using Pearson or Spearman correlation coefficients.

Additional methods are provided in the supplemental Methods. All reagents used are enclosed as Supplemental Table 3.

RESULTS

SCD levels are prognostic in AML and its inhibition induces cell death in a subset of AML cell lines

Analysis of multiple independent gene expression profiles of newly diagnosed AML samples shows that higher levels of *SCD* expression correlate with significantly decreased survival even after correcting for age, gender and European Leukemia Net (ELN) prognostic group (Fig 1A-B). This finding was confirmed when analysing a local cohort of patients with adverse risk AML (Suppl. Fig 1A). High *SCD* expression correlates with several genes involved in FAS and desaturation such as fatty acid synthase (*FASN)*, fatty acid desaturase 1 and 2 (*FADS1* and *FADS2)* and adverse prognostic features

such as *TP53* mutant signatures and the leukemic stem cell signature – LSC17[22] (Fig 1C, Ext. 1B). A biosynthesis of unsaturated FA gene signature is enriched in matched post-chemotherapy relapse versus diagnosis in human AML samples (Fig 1D and Suppl. Fig1C), together with a TCGA-generated SCD signature (Fig 1E). Interestingly, SCD signature was inversely correlated with tumour burden in Ara-C-treated PDX models[13] and was significantly upregulated at nadir after chemotherapy (minimal residual disease, MRD) (Fig 1F). Overall these data suggest that synthesis of unsaturated FA is more active at points of leukaemia resistance or progression raising the possibly that SCD is linked with mechanisms regulating sensitivity to chemotherapy. To test SCD as a therapeutic target, we used the clinical grade SCD inhibitor SSI-4 against a panel of human AML cell lines. SSI-4 induced cell death in several cell lines (K562, MOLM-13, MV-4-11), while others (OCI-AML3, THP-1, HL-60, Kasumi-1 and TF-1) were resistant (Fig 1G). SSI-4 anti-leukemic effects were a result of cell death induction, as no effects on cell cycle progression were observed and sensitivity to SSI-4 was not associated to any mutational characteristics of the cell lines tested (Suppl. Fig 1D-E).

We validated these data using another SCD inhibitor A939572 (Suppl. Fig 2A). Moreover, SCD genetic depletion rapidly impaired growth in SSI-4-sensitive cells (Suppl. Fig 2B) but did not decrease cell viability in standard culture conditions , possibly due to compensatory upregulation of other fatty acid desaturases[23]. However, when cells were grown in hypoxic conditions, which are known to increase FAS and dependency on SCD[24], SCD depletion induced cell death specifically in SSI-4 sensitive cells (Suppl. Fig2C-D).

SCD activity dictates sensitivity to SCD inhibition by preventing SFA accumulation and lipotoxicity

Since genetic features did not correlate with sensitivity to SCD inhibition, we analysed publicly available proteomic data[25] for SSI-4 sensitive and resistant cell lines. These showed an enrichment in adipogenesis signature and higher SCD protein expression in sensitive cells (Fig 2A-B) . Western blot analysis confirmed these findings, suggesting a greater dependency on fatty acid desaturation in sensitive cells (Fig 2C-D). Fatty acid quantitation showed that the SFA/MUFA ratio is significantly higher in resistant cell lines when compared to sensitive ones. However, the expected increase in ratio upon SSI-4 treatment is much lower in the resistant OCI-AML3 compared to the sensitive cells, indicating lower dependency on SCD activity in resistant cells (Fig 2E-F). Conversely sensitivity to SCD inhibition did not correlate with uptake of external lipids, or expression of lipid transporters CD36 and LDLR (Suppl. Fig 2E), both previously identified as independent prognostic factors in AML[26,27]. Gas chromatography-mass spectrometry (GC/MS) experiments tracing uniformly-labelled ^{13}Carbon (U-$^{13}C_6$) glucose incorporation into FA demonstrated that in sensitive cells MUFA biosynthesis (16:1, C18:1) was higher and more responsive to SCD inhibition. Interestingly, treatment with SSI-4 also led to increased production of SFA stearate (C18:0) in sensitive cells. Together these data suggest that SSI-4 sensitive cells have a more active *de novo* fatty acid biosynthesis and desaturation which is further increased upon SCD inhibition. Enhanced FAS is however uncoupled from desaturation following SSI-4 treatment thus causing an imbalance between SFA and MUFA levels to a degree able to trigger lipotoxicity[28] and cell death (Fig 2F-G).

MUFA and SFA levels modulate sensitivity to SCD inhibition in AML cells by regulating FAS

The above data suggest that, in cells sensitive to SCD inhibition, MUFA production is a sensing point for FAS pathway activity. To test this hypothesis, we grew cells in the presence of oleate and noted decreased production of both SFA and MUFA (Fig 3A and Suppl. Fig 3A-B) which also correlated with a complete rescue of SSI-4-mediated decrease in viability, supporting the on-target efficacy of SSI-4 (Fig 3B). Conversely, addition of palmitate in non-toxic concentration increased FAS and oleate production mostly in resistant, but not sensitive cells (Fig 3C and Suppl. Fig 3A-B). This suggests that

baseline MUFA production in resistant cells is below its potential maximum and can be upregulated following palmitate supplementation. Although exogenous palmitate can still be detoxified by desaturation both in sensitive and resistant cells, as shown by total levels of labelled and unlabelled MUFA (Suppl. Fig3B), in palmitate rich conditions, SCD inhibition results in a large increase in the SFA/MUFA ratio. This is true even in resistant cells that do not display such strong imbalance upon treatment with SSI-4 alone (Fig. 2E, Suppl. Fig 3A-C) and causes increased sensitivity to SSI-4 in both sensitive and resistant cells in the presence of palmitate (Fig 3D).

These data demonstrate that changes in MUFA/SFA levels affect sensitivity to SCD inhibition via modulation of FAS. To clarify the mechanistic underpinning of this observation we analysed changes in regulatory pathways of FAS in sensitive cells. Consistent with the observed increase in the FAS rate, SCD inhibition reduced activation of AMPK (Fig 3E), thereby relieving its inhibitory role on cleavage and consequent activation of SREBP2 (Fig 3F), a key transcription factor modulating FAS enzymes expression[29,30]. As expected following SREBP2 activation, we observed increased levels of FASN, SCD (Fig 2C and 3F) and total acetyl-Coa carboxylase (ACC) which were reversed by the addition of oleate, thus confirming that MUFA levels relieve SCD inhibition toxicity through downregulation of FAS (Fig 3F, Suppl. Fig 4A). Conversely, the AMPK activator MK-8722 decreased both SREBP2 cleavage and expression of SCD and FASN (Fig 3G). Although SREBP2 has mostly been described as a regulator of cholesterol synthesis, while FAS is generally under regulation of SREBP1[30], in our system we observed more consistent effects on SREBP2 following SCD inhibition and MUFA addition. Conversely, we did not see a change in SREBP1 cleavage in response to SSI-4, with or without the addition of oleate, even though AMPK activation with MK-8722 decreased SREBP1 cleavage as expected (Suppl. Fig 4B). These data suggest that FAS in AML cell lines is prominently regulated by SREBP2, as shown in other models[31].

Decreasing FAS by inhibition of either FASN or ACC or via AMPK activation abolished SSI-4 mediated toxicity (Fig 3H, Suppl. Fig 4B-C). Interestingly, analysis of the Depmap dataset shows that SCD dependency inversely correlates with the expression levels of both *FASN* and *ACACA* (ACC) across all cancer cells lines and particularly AML ones (Suppl. Fig 4D). Overall these data confirm that modulation of FAS impacts sensitivity to SCD inhibition.

Cell death in response to SSI-4 is mediated by lipid oxidative stress, integrated stress response and activation of apoptotic machinery.

Transcriptomic analysis of SSI-4 treated cells confirmed the regulatory role of oleate levels on the rate of FAS but also identified oxidative stress associated pathways (ferroptosis, glutathione metabolism) and integrated stress/endoplasmic reticulum (ER) stress response as potential downstream mechanisms leading to cell death (Fig 4A and Suppl. Fig 5A).

Consistent with SCD role in protection against oxidative stress and lipid peroxidation[20], sensitive cells displayed a specific increase in lipid peroxidation as measured by Bodipy C11 staining upon treatment with SSI-4 (Fig 4B). A similar effect was observed in cells with downregulated SCD in hypoxic condition where lipotoxicity is present (Suppl. Fig 5B). Lipidomic analysis confirmed that lysophospholipids which have lost their polyunsaturated tail, a known marker of lipid peroxidation[32], are the most enriched lipid class in response to SSI-4 (Fig 4C). This pattern was completely abrogated by the addition of oleate (Suppl. Fig 5C). However, despite reducing peroxidation to the same extent of oleate (Suppl. Fig 5D-E), lipid peroxidation inhibitors failed to or only partially rescued (Fig 4D and Suppl. Fig 5F-G) sensitive cells from SSI-4-mediated cell death. Reversal of lipid peroxidation is therefore not sufficient to prevent cell death induced by SCD inhibition.

SCD is essential for ER homeostasis[33] and SFA/MUFA imbalance is known to trigger ER stress[34]. Based on our transcriptomic data, we interrogated the three arms of the ER response pathway (Suppl. Fig 6A). We noticed a substantial increase in targets downstream of PERK, CHOP and ATF4, a moderate increase in IRE1 and IRE1-associated targets, spliced and total XBP1, and no effects on the expression of ATF6. In accordance to that, PERK inhibitor GSK2656157 rescued SSI-4-mediated cytotoxicity, while IRE1 inhibitor 4μ8c demonstrated only milder cytoprotective effects at higher doses and ATF6 inhibitor Ceapin A7 had no effects (Suppl. Fig 6B). The PERK pathway is a known regulator of apoptosis[35] and SSI-4 treatment induced accumulation of apoptotic marker Annexin V and activation of apoptotic machinery in both sensitive cells and resistant ones grown in the presence of palmitate (Fig 4E-F). Still, in contrast to oleate supplementation, co-treatment with pan-caspase inhibitor Q-Vd-OPh resulted in a significant, but only partial rescue of SSI-4 mediated cell death (Fig 4F-G).

Overall these data show that the lipotoxic reaction in response to SSI-4 cannot be reduced to the activation of a single effector death mechanism. Indeed SCD inhibition has been shown in other models to act as a pleiotropic trigger which can activate several cell death modes concurrently, thus explaining the detection of both ferroptosis or apoptosis markers[36]. Consistent with this, inhibiting any of these cell death mechanisms independently did not completely rescue the cytotoxic effects of SSI-4 supporting their functional redundance.

Primary AML cells with higher levels of unsaturated fatty acids are sensitive to SCD inhibition.

To extend the translational relevance of our findings, we tested the effects of SSI-4 on primary AML samples *in vitro*. First, we observed that co-culture of primary AML samples with MS-5 cells decreased sensitivity to SSI-4 and abolished palmitate-mediated toxicity, suggesting that the presence of stroma could influence SCD dependency (Suppl. Fig 7A). We thus treated 36 primary AML samples in stromal co-culture with SSI-4 and observed that, similar to cell lines, primary samples dichotomized into sensitive and resistant (Fig 5A), with no clear relation to specific driver mutations (Suppl. Table 1). This was confirmed on an independent cohort of 11 primary samples (Suppl. Fig 7C). We did not identify a sensitivity signature using transcriptomic or proteomic approaches (data not shown), while phosphoproteomic data on a subset of AML patient samples showed significantly higher levels of phosphorylated-insulin receptor substrate 2 (IRS2) in sensitive cells (Fig 5B) which was confirmed in an independent phosphoproteomic analysis on a different patient sample subset (Suppl. Fig 7D). IRS2 is a downstream target of receptor tyrosine kinases (RTK) and has been shown to specifically regulate the insulin-like growth factor-1 (IGF-1) autocrine production and signalling in AML[37]. The activation of RTK was further supported by increased phosphorylation of AKT2 and PLEKHG3 (Suppl. Fig 7E). Interestingly, increased activation of signalling downstream of RTK in this AML model did not correlate with faster progression through cell cycle (Suppl. Fig 7F) suggesting that sensitivity is not linked to a more proliferative phenotype, but potentially to the role of RTKs in regulation of lipogenesis and energy metabolism[38]. Indeed, in accordance with cell line data, sensitive samples displayed higher levels of MUFAs and a lower SFA/MUFA ratio compared to resistant cells supporting their greater dependency on fatty acid desaturation (Fig 5C-D).

Given the observed stromal protection towards SSI-4-mediated toxicity, we tested to which extent the anti-leukemic effect of SCD inhibition was maintained *in vivo* using patient derived xenografts (PDX) from two sensitive AML samples . A significant decrease in bone marrow (BM) leukaemia burden following SSI-4 treatment was observed in one PDX model and higher levels of lipid peroxidation in the human $CD45^+$ compartment were noted following SSI-4 even when leukemic burden was not significantly reduced (Fig 5E-F and Suppl. Fig 7G). This suggests that SCD inhibition primes AML cells to aberrant oxidative stress *in vivo* even when its antileukemic effects are blunted.

SSI-4 does not affect normal haematopoiesis, but as a single agent does not prolong survival in iMLL-AF9 murine AML model.

Although a favourable general toxicity profile of SSI-4 was demonstrated in previous animal studies [6,21], we also ascertained its potential hematopoietic toxicity. SSI-4 had no significant hematopoietic toxicity, as shown by its effects on the peripheral blood (PB) counts and hematopoietic progenitor compartments of treated animals (Fig 6A-B).

We then assessed the effects of SCD inhibition in two AML murine models expressing either the *Hoxa9/Meis1* or inducible *MLL-AF9* (*iMLL-AF9*) oncogene. Both models were sensitive *in vitro* to SSI-4 with toxicity reversed by addition of oleate (Fig 6C-D). However, *in vivo* treatment of *iMLL-AF9* model with SSI-4 resulted only in induction of differentiation without significant decrease in BM leukemic burden(Fig 6E). Indeed, SSI-4 did not prolong survival in this model although, as seen in PDX, increased lipid peroxidation in AML cells *in vivo* (Fig 6F-H).

SSI-4 combination with doxorubicin based chemotherapy is synergistic and prolongs survival in murine AML models

Lipid peroxidation is the most consistent phenotype observed in response to SSI-4 across all AML models tested and is known to induce DNA damage[39] through production of malondialdehyde which forms DNA adducts in normal and oncogenic mammalian cells[40]. Moreover a role of SCD inhibition in modulating DNA damage repair via downregulation of RAD51 has already been reported[33]. In sensitive cells, a strong lipotoxic phenotype upon combined treatment with palmitate and SSI-4 induced DNA damage as measured by phosphorylated histone H2A.X (Fig 7A). This prompted us to assess the therapeutic potential of SSI-4 combination with the DNA-damaging chemotherapeutic doxorubicin. Indeed SSI-4 increased doxorubicin induced DNA damage (Fig 7B) with similar effects on lipid peroxidation (Suppl. Fig 8A). Moreover SCD depletion resulted in growth disadvantage in the presence of doxorubicin and increased sensitivity to doxorubicin-induced cytotoxicity (Fig 7C and Suppl. Fig 8B). The relevance of the SFA/MUFA ratio and induction of lipotoxicity in modulating AML cells sensitivity to anthracycline is further supported by the observation that inhibition of palmitate production using a FASN inhibitor or AMPK activation reduces sensitivity to doxorubicin alone or in combination with SSI-4 (Suppl. Fig 8C).

We detected synergism between SSI-4 and doxorubicin in MV-4-11 cells at the majority of dose combinations, while in *iMLL-AF9* cells, which displayed greater sensitivity to doxorubicin, synergy was evident when doxorubicin was applied in lower concentrations (Fig 7D). Moreover, analysis of the BeatAML dataset showed that higher *SCD* expression correlates with reduced sensitivity *in vitro* to cytarabine, an antimetabolite known to cause DNA damage and used in combination with anthracyclines to treat AML patients (Suppl. Fig 8D). Finally, to validate these findings *in vivo* we used two aggressive models of fully established AML that are more representative of the scenario routinely encountered in clinic, a cell line derived xenograft (CDX) and a transplant of leukemic *iMLL-AF9* cells. The latter reached an average leukemic blasts infiltration in PB of 20% before treatment (Suppl. Fig 8E), a common criterion for AML diagnosis. Similarly to what we observed in the PDX, response to SSI-4 therapy as a single agent was varied with significant survival improvement in the CDX model but not in the murine *iMLL-AF9* model. However in both models and consistent with the *in vitro* findings, combining SSI-4 treatment with doxorubicin and cytarabine, a protocol mimicking the standard intensive chemotherapy used in patients, significantly prolonged survival (Fig 7E-F). Together these results demonstrate that SCD inhibition augments efficacy of standard AML chemotherapy likely by enhancing their ability to induce DNA damage.

DISCUSSION

In this work we sought to understand AML metabolic reliance on FAS to uncover novel vulnerabilities that could be tested clinically. Consistent with observations in several solid cancers[41-43], high SCD expression is an independent adverse prognostic marker in AML. The prognostic role of SCD is likely due to its association with sensitivity to chemotherapy given that biosynthesis of unsaturated fatty acids is enriched in relapsed and chemo-refractory patients. The latter observation emphasizes the potential of SCD inhibition as a treatment strategy in AML particularly when combined with standard chemotherapy. Indeed our data, together with those of previous studies suggesting a role for SCD in protecting AML cells from novel targeted therapies[20] or experimental agents[19] , support SCD inhibition as a promising candidate for combinatorial pharmacological approaches.

The greatest challenge in targeting SCD has been the lack of available clinical grade inhibitors[17]. SSI-4 is under clinical development for hepatocellular carcinoma[6], and in our study demonstrated potent anti-leukemic effects *in vitro* on a subset of AML samples while showing no general or hematopoietic toxicities. Although it is often shown that the effects of SCD inhibition are more pronounced in lipid depleted environment[8,44], i.e. cerebrospinal fluid[18], in our models we observed a strong decrease in viability of sensitive AML cells in standard experimental conditions, suggesting they are unable to take advantage of the extracellular lipid provision available to them.

Although specific mutations can dictate selective metabolic vulnerabilities[45-47], metabolic dependencies can be present across multiple genetic backgrounds as a phenotype bottleneck i.e. a state essential for continued tumorigenesis. This can be advantageous as metabolic vulnerabilities can be exploited in a larger proportion of patients in a mutation-agnostic manner. This also highlights the challenge to identify determinants of sensitivity, so that each therapy is used in patients most likely to benefit while sparing its toxicity to those unlikely to respond. This is crucial for metabolic inhibitors as they often target pathways central to the function of normal cells/tissues. Indeed, despite several metabolic inhibitors have progressed to early phase clinical trials[48], most of these have failed to improve patients outcome[5]. This is likely linked to distinct metabolic dependencies of different tumour subtypes and/or heterogeneity even within individual tumours.

We indeed observed that both AML cell lines and primary samples clearly dichotomized in sensitive and resistant to SCD inhibition, a pattern also observed in glioblastoma and melanoma[7,49,50]. Sensitivity to SSI-4 was not related to mutational background, instead, sensitive cells displayed both greater *de novo* MUFA production and higher MUFA levels. Sensitive cells showed greater dependency on FA desaturation and SCD inhibition caused a greater SFA/MUFA imbalance resulting in lipotoxicity. Moreover SCD appears to be the regulatory nexus of *de novo* FAS in AML cells, because oleate decreases FAS both in resistant and sensitive cells, rescuing SSI-4-mediated toxicity both by replenishing the MUFA pool, but also preventing SFA production. Moreover, SCD inhibition in sensitive cells increases SFA production, most likely through a feedback loop that relieves inhibitory effects of AMPK on FAS, which further potentiates SFA/MUFA imbalance. Similar effects were observed in pancreatic duct adenocarcinoma (PDAC) cells where exposure to oleate in delipidated medium also decreased FA production, irrespective of SCD inhibition, and inhibition of SFA production rescued toxicity of SCD inhibition, consistent with our model[51]. Moreover in the same study, caloric restriction diet impaired tumour growth in a PDAC mouse model through upregulation of *de novo* FAS and concomitant decrease in SCD activity leading to SFA/MUFA imbalance, which could again be rescued by the presence of exogenous lipids.

Therefore based on the literature and our data, several important considerations can be made. First to drive cytotoxicity via SCD inhibition a significant imbalance between SFA/MUFA needs to be

generated. This could be achieved by modulating the diet, either through a palmitate rich or a caloric restricted diet, which creates a dependency on FAS and reduces SCD levels[51]. This will be the focus of future work. Conversely, therapeutic interventions which inhibit FAS might reduce the efficacy of SCD inhibition and should be avoided in this setting. Interestingly, this is consistent with gene knockout fitness profile data identifying tumour suppressor roles for genes involved in saturated FAS, i.e. FASN and ACC, in a subset of AML, while highlighting fatty acid desaturation and SCD as a therapeutic vulnerability in the same group, further supporting our findings[52]. Interestingly in the same study a transcriptional signature in paediatric AML cases based on the expression of genes involved in saturated FAS was shown to be prognostic and, we speculate, likely to predict sensitivity to SCD inhibition. We did not detect a transcriptional signature of sensitivity but noted that sensitive primary AML samples displayed increased phosphorylation of IRS2, a direct downstream target of insulin and growth factor receptors[53]. Insulin is a known regulator of SCD expression[54], and sensitivity to SCD inhibition in glioblastoma has been linked to increased ERK phosphorylation[7], also a downstream target of RTK signaling[55], while FLT3 inhibition in AML decreases MUFA levels through SCD downregulation[20]. Interestingly, all the sensitive cell lines in our study harboured mutations associated with increased RTK signalling (*BCR-ABL*, *FLT3*) and resistant cell lines presented with *NRAS* mutation, that is known to decrease sensitivity to SCD in solid cancer models[56]. However, these observations could not be replicated in our primary samples cohort, again highlighting the complexity of interactions between mutational profiles and signalling mechanisms in AML[57]. Although our data indicate that sensitivity to SCD inhibition might correlate with levels of RTK signalling, further work on larger patient cohorts is required to confirm this as a predictive biomarker of response.

The exact mechanism through which lipotoxicity induces cell death remains ill-defined. A previous report studying the molecular basis of palmitate-induced cell death, predominantly ascribed its effects to induction of ER stress, and pharmacological modulators of ER stress-related signalling pathways could partially alleviate palmitate-toxicity[34]. Conversely, reduction of MUFAs is a known inducer of ferroptotic cell death[58]. In response to SCD inhibition we observed pleiotropic effects causing both increased ER stress with activation of transcription factor DDIT3/CHOP and apoptotic machinery and elevated lipid peroxidation which is a hallmark of ferroptosis[32]. However, inhibition of each of these pathways alone could achieve only a partial rescue of SSI-4-mediated cell death, indicating their functional redundancy. Indeed it has already been shown in glioma cells that SCD inhibition results in distinct downstream effects[28] and both apoptotic and ferroptotic cell death pathways are triggered in response to SCD inhibition in ovarian cancer[36]. These conclusions are further supported by the observation that oleate supplementation, which can fully rescue viability of SSI-4 treated cells, acts in parallel on FAS, lipid peroxidation, ER stress and apoptosis, in accordance with its already known ability to rescue both apoptotic and ferroptotic cell death in response to SFA accumulation[59].

The ability of exogenous MUFA to rescue SCD-mediated impairment in tumour growth, both shown *in vitro* in our study and *in vivo* in a murine PDAC model[51], suggested a potential stromal protection against anti-leukemic effects of SSI-4. Indeed, SSI-4 toxic effects were less pronounced when primary AML cells were grown in co-culture with stroma and were only partially maintained *in vivo*. As expected, and comparable to what is described in glioblastoma[7], SSI-4 as a single agent did not consistently prolong survival in AML mouse models. Still, increased lipid peroxidation as a marker of SCD inhibition was maintained even when the decrease in leukemic burden was not prominent, indicating that SSI-4 treated leukemic cells are primed for a second cytotoxic hit. In our models lipotoxicity was linked with increased DNA damage, consistent with what was seen in glioblastoma[7], and oxidative stress-inducing strategies have been shown to enhance the response to chemotherapy in AML[60]. Indeed, we observed synergy between SCD inhibition and doxorubicin *in vitro* and combination of SSI-4 with conventional AML chemotherapy in two aggressive AML models *in vivo*

significantly prolonged survival. These findings highlight that genuinely lethal metabolic bottlenecks are often generated by the action of already approved therapeutic interventions and metabolic vulnerabilities can be fully exploited via synergistic combination therapies [20,61,62].

In conclusion our findings support the efforts of devising new treatment approaches in AML focusing on the metabolic axis of MUFA synthesis. Going forward, as will be the case for most metabolic inhibitors, further research on the identification of predictive biomarkers of response and novel combination approaches, with either other approved therapies or dietary interventions, are essential for fully realising the potential of targeting this axis in AML.

Acknowledgements

We would like to thank Dora Visnjic for helpful advice and discussion and Han Tun and Justyna Gleba for critically reading the manuscript. We wish to thank the Barts Cancer Institute tissue bank for sample collection and processing. This research was supported by the BCI Flow cytometry facility (CRUK Core Award C16420/A18066). This work was supported by the Cancer Research UK (PG, Advanced Clinician Scientist fellowship, C57799/A27964) and The Lady Tata Memorial Trust (VD, International Award for Research in Leukaemia). All diagrams and illustrations were created using Biorender.com.

Author contributions (CredIT):

Conceptualization: PG and VD. Methodology: VD, HL, RB, CP, MA, GRB, AvK, BP, JES, JT, AF, JAC, BP (2), KK, PG. Validation: LO. Formal analysis: ARM, PCI, FBC, DPM, GRB, EB. Investigation: VD, HL, RB, CP, SJ, SA, JD, LW, JC, AM, KW, MA, GRB, LO. Resources: CP, JES, JS, JT, JJS, LH, JAC, MY, PC, JF, KRP, KK, PG. Writing – original draft: VD, PG. Writing – review and editing: all authors. Visualization: VD, PG. Supervision: KRP, KK, PG. Project administration: PG. Funding acquisition: AvK, PC, JF, KK, PG.

Confilct of interests

LH is CEO and co-founder of Modulation Therapeutics, the company holding intellectual property to SSI-4. J.A.C. holds a patent regarding use of the SCD inhibitor SSI-4.

References

1. DiNardo CD, Erba HP, Freeman SD, Wei AH. Acute myeloid leukaemia. *The Lancet*. doi:10.1016/S0140-6736(23)00108-3
2. Zeng AGX, Bansal S, Jin L, et al. A cellular hierarchy framework for understanding heterogeneity and predicting drug response in acute myeloid leukemia. *Nature Medicine*. 2022/06/01 2022;28(6):1212-1223. doi:10.1038/s41591-022-01819-x
3. Papaemmanuil E, Gerstung M, Bullinger L, et al. Genomic Classification and Prognosis in Acute Myeloid Leukemia. *New England Journal of Medicine*. 2016/06/09 2016;374(23):2209-2221. doi:10.1056/NEJMoa1516192
4. Culp-Hill R, D'Alessandro A, Pietras EM. Extinguishing the Embers: Targeting AML Metabolism. *Trends in Molecular Medicine*. 2021/04/01/ 2021;27(4):332-344. doi:https://doi.org/10.1016/j.molmed.2020.10.001
5. Yap TA, Daver N, Mahendra M, et al. Complex I inhibitor of oxidative phosphorylation in advanced solid tumors and acute myeloid leukemia: phase I trials. *Nature Medicine*. 2023/01/01 2023;29(1):115-126. doi:10.1038/s41591-022-02103-8
6. Ma MKF, Lau EYT, Leung DHW, et al. Stearoyl-CoA desaturase regulates sorafenib resistance via modulation of ER stress-induced differentiation. *Journal of Hepatology*. 2017/11/01/ 2017;67(5):979-990. doi:https://doi.org/10.1016/j.jhep.2017.06.015
7. Eyme KM, Sammarco A, Jha R, et al. Targeting de novo lipid synthesis induces lipotoxicity and impairs DNA damage repair in glioblastoma mouse models. *Science Translational Medicine*. 15(679):eabq6288. doi:10.1126/scitranslmed.abq6288
8. Peck B, Schug ZT, Zhang Q, et al. Inhibition of fatty acid desaturation is detrimental to cancer cell survival in metabolically compromised environments. *Cancer & Metabolism*. 2016/04/01 2016;4(1):6. doi:10.1186/s40170-016-0146-8
9. Li J, Condello S, Thomes-Pepin J, et al. Lipid Desaturation Is a Metabolic Marker and Therapeutic Target of Ovarian Cancer Stem Cells. *Cell Stem Cell*. 2017/03/02/ 2017;20(3):303-314.e5. doi:https://doi.org/10.1016/j.stem.2016.11.004
10. Samudio I, Harmancey R, Fiegl M, et al. Pharmacologic inhibition of fatty acid oxidation sensitizes human leukemia cells to apoptosis induction. *The Journal of Clinical Investigation*. 01/04/ 2010;120(1):142-156. doi:10.1172/JCI38942
11. Stevens BM, Jones CL, Pollyea DA, et al. Fatty acid metabolism underlies venetoclax resistance in acute myeloid leukemia stem cells. *Nature Cancer*. 2020/12/01 2020;1(12):1176-1187. doi:10.1038/s43018-020-00126-z
12. Tcheng M, Roma A, Ahmed N, et al. Very long chain fatty acid metabolism is required in acute myeloid leukemia. *Blood*. 2021;137(25):3518-3532. doi:10.1182/blood.2020008551
13. Farge T, Saland E, de Toni F, et al. Chemotherapy-Resistant Human Acute Myeloid Leukemia Cells Are Not Enriched for Leukemic Stem Cells but Require Oxidative Metabolism. *Cancer Discovery*. 2017;7(7):716-735. doi:10.1158/2159-8290.CD-16-0441
14. Schulze PC, Drosatos K, Goldberg IJ. Lipid Use and Misuse by the Heart. *Circulation Research*. 2016/05/27 2016;118(11):1736-1751. doi:10.1161/CIRCRESAHA.116.306842
15. Holubarsch Christian JF, Rohrbach M, Karrasch M, et al. A double-blind randomized multicentre clinical trial to evaluate the efficacy and safety of two doses of etomoxir in comparison with placebo in patients with moderate congestive heart failure: the ERGO (etomoxir for the recovery of glucose oxidation) study. *Clinical Science*. 2007;113(4):205-212. doi:10.1042/CS20060307
16. Ntambi JM, Miyazaki M. Regulation of stearoyl-CoA desaturases and role in metabolism. *Progress in Lipid Research*. 2004/03/01/ 2004;43(2):91-104. doi:https://doi.org/10.1016/S0163-7827(03)00039-0
17. Tracz-Gaszewska Z, Dobrzyn P. Stearoyl-CoA Desaturase 1 as a Therapeutic Target for the Treatment of Cancer. *Cancers*. 2019;11(7). doi:10.3390/cancers11070948

18. Savino AM, Fernandes SI, Olivares O, et al. Metabolic adaptation of acute lymphoblastic leukemia to the central nervous system microenvironment depends on stearoyl-CoA desaturase. *Nature Cancer*. 2020/10/01 2020;1(10):998-1009. doi:10.1038/s43018-020-00115-2
19. Subedi A, Liu Q, Ayyathan DM, et al. Nicotinamide phosphoribosyltransferase inhibitors selectively induce apoptosis of AML stem cells by disrupting lipid homeostasis. *Cell Stem Cell*. 2021/10/07/ 2021;28(10):1851-1867.e8. doi:https://doi.org/10.1016/j.stem.2021.06.004
20. Sabatier M, Birsen R, Lauture L, et al. C/EBPa confers dependence to fatty acid anabolic pathways and vulnerability to lipid oxidative stress-induced ferroptosis in FLT3-mutant leukemia. *Cancer Discovery*. 2023:CD-22-0411. doi:10.1158/2159-8290.CD-22-0411
21. von Roemeling CA, Caulfield TR, Marlow L, et al. Accelerated bottom-up drug design platform enables the discovery of novel stearoyl-CoA desaturase 1 inhibitors for cancer therapy. *Oncotarget; Vol 9, No 1*. 2017;
22. Ng SWK, Mitchell A, Kennedy JA, et al. A 17-gene stemness score for rapid determination of risk in acute leukaemia. *Nature*. 2016/12/01 2016;540(7633):433-437. doi:10.1038/nature20598
23. Vriens K, Christen S, Parik S, et al. Evidence for an alternative fatty acid desaturation pathway increasing cancer plasticity. *Nature*. 2019/02/01 2019;566(7744):403-406. doi:10.1038/s41586-019-0904-1
24. Melana JP, Mignolli F, Stoyanoff T, et al. The Hypoxic Microenvironment Induces Stearoyl-CoA Desaturase-1 Overexpression and Lipidomic Profile Changes in Clear Cell Renal Cell Carcinoma. *Cancers*. 2021;13(12). doi:10.3390/cancers13122962
25. Nusinow DP, Szpyt J, Ghandi M, et al. Quantitative Proteomics of the Cancer Cell Line Encyclopedia. *Cell*. 2020/01/23/ 2020;180(2):387-402.e16. doi:https://doi.org/10.1016/j.cell.2019.12.023
26. Perea G, Domingo A, Villamor N, et al. Adverse prognostic impact of CD36 and CD2 expression in adult de novo acute myeloid leukemia patients. *Leukemia Research*. 2005/10/01/ 2005;29(10):1109-1116. doi:https://doi.org/10.1016/j.leukres.2005.02.015
27. Floeth M, Elges S, Gerss J, et al. Low-density lipoprotein receptor (LDLR) is an independent adverse prognostic factor in acute myeloid leukaemia. https://doi.org/10.1111/bjh.16853. *British Journal of Haematology*. 2021/02/01 2021;192(3):494-503. doi:https://doi.org/10.1111/bjh.16853
28. Williams KJ, Argus JP, Zhu Y, et al. An Essential Requirement for the SCAP/SREBP Signaling Axis to Protect Cancer Cells from Lipotoxicity. *Cancer Research*. 2013;73(9):2850-2862. doi:10.1158/0008-5472.CAN-13-0382-T
29. Li Y, Xu S, Mihaylova MM, et al. AMPK Phosphorylates and Inhibits SREBP Activity to Attenuate Hepatic Steatosis and Atherosclerosis in Diet-Induced Insulin-Resistant Mice. *Cell Metabolism*. 2011/04/06/ 2011;13(4):376-388. doi:https://doi.org/10.1016/j.cmet.2011.03.009
30. Shimano H, Sato R. SREBP-regulated lipid metabolism: convergent physiology — divergent pathophysiology. *Nature Reviews Endocrinology*. 2017/12/01 2017;13(12):710-730. doi:10.1038/nrendo.2017.91
31. Vergnes L, Chin RG, de Aguiar Vallim T, et al. SREBP-2-deficient and hypomorphic mice reveal roles for SREBP-2 in embryonic development and SREBP-1c expression [S]. *Journal of Lipid Research*. 2016;57(3):410-421. doi:10.1194/jlr.M064022
32. Yang WS, Stockwell BR. Ferroptosis: Death by Lipid Peroxidation. *Trends in Cell Biology*. 2016/03/01/ 2016;26(3):165-176. doi:https://doi.org/10.1016/j.tcb.2015.10.014
33. Pinkham K, Park DJ, Hashemiaghdam A, et al. Stearoyl CoA Desaturase Is Essential for Regulation of Endoplasmic Reticulum Homeostasis and Tumor Growth in Glioblastoma Cancer Stem Cells. *Stem Cell Reports*. 2019/04/09/ 2019;12(4):712-727. doi:https://doi.org/10.1016/j.stemcr.2019.02.012
34. Piccolis M, Bond LM, Kampmann M, et al. Probing the Global Cellular Responses to Lipotoxicity Caused by Saturated Fatty Acids. *Molecular Cell*. 2019/04/04/ 2019;74(1):32-44.e8. doi:https://doi.org/10.1016/j.molcel.2019.01.036

35. Oakes SA, Papa FR. The Role of Endoplasmic Reticulum Stress in Human Pathology. *Annual Review of Pathology: Mechanisms of Disease*. 2015/01/24 2015;10(1):173-194. doi:10.1146/annurev-pathol-012513-104649
36. Tesfay L, Paul BT, Konstorum A, et al. Stearoyl-CoA Desaturase 1 Protects Ovarian Cancer Cells from Ferroptotic Cell Death. *Cancer Research*. 2019;79(20):5355-5366. doi:10.1158/0008-5472.CAN-19-0369
37. Tamburini J, Chapuis N, Bardet V, et al. Mammalian target of rapamycin (mTOR) inhibition activates phosphatidylinositol 3-kinase/Akt by up-regulating insulin-like growth factor-1 receptor signaling in acute myeloid leukemia: rationale for therapeutic inhibition of both pathways. *Blood*. 2008;111(1):379-382. doi:10.1182/blood-2007-03-080796
38. Jin N BA, Lan X, Xu J, Wang X, Liu Y, Wang T, Tang S, Zeng H, Chen Z, Tan M, Ai J, Xie H, Zhang T, Liu D, Huang R, Song Y, Leung EL, Yao X, Ding J, Geng M, Lin SH, Huang M. Identification of metabolic vulnerabilities of receptor tyrosine kinases-driven cancer *Nature Communications*. 2019;10(1):2701. doi:doi: 10.1038/s41467-019-10427-2.
39. Gentile F, Arcaro A, Pizzimenti S, et al. DNA damage by lipid peroxidation products: implications in cancer, inflammation and autoimmunity. *AIMS Genet*. 08.2017 2017;04(02):103-137. doi:10.3934/genet.2017.2.103
40. Marnett LJ. Oxy radicals, lipid peroxidation and DNA damage. *Toxicology*. 2002/12/27/ 2002;181-182:219-222. doi:https://doi.org/10.1016/S0300-483X(02)00448-1
41. Wang C SM, Ji J, Cai Q, Zhao Q, Jiang J, liu J, Zhang H, Zhu Z, Zhang J. Stearoyl-CoA desaturase 1 (SCD1) facilitates the growth and anti-ferroptosis of gastric cancer cells and predicts poor prognosis of gastric cancer. *Aging (Albany NY)*. 2020;12:15374-15391. doi: https://doi.org/10.18632/aging.103598
42. Wang J, Xu Y, Zhu L, et al. High Expression of Stearoyl-CoA Desaturase 1 Predicts Poor Prognosis in Patients with Clear-Cell Renal Cell Carcinoma. *PLOS ONE*. 2016;11(11):e0166231. doi:10.1371/journal.pone.0166231
43. Ran H, Zhu Y, Deng R, et al. Stearoyl-CoA desaturase-1 promotes colorectal cancer metastasis in response to glucose by suppressing PTEN. *Journal of Experimental & Clinical Cancer Research*. 2018/03/12 2018;37(1):54. doi:10.1186/s13046-018-0711-9
44. Yuki K, Tomonori Y, Akiko K, et al. Inhibition of stearoyl-CoA desaturase 1 (SCD1) enhances the antitumor T cell response through regulating β-catenin signaling in cancer cells and ER stress in T cells and synergizes with anti-PD-1 antibody. *Journal for ImmunoTherapy of Cancer*. 2022;10(7):e004616. doi:10.1136/jitc-2022-004616
45. Dembitz V, Gallipoli P. The Role of Metabolism in the Development of Personalized Therapies in Acute Myeloid Leukemia. Mini Review. *Frontiers in Oncology*. 2021-May-19 2021;11doi:10.3389/fonc.2021.665291
46. Fenouille N, Bassil CF, Ben-Sahra I, et al. The creatine kinase pathway is a metabolic vulnerability in EVI1-positive acute myeloid leukemia. *Nature Medicine*. 2017/03/01 2017;23(3):301-313. doi:10.1038/nm.4283
47. Liu J, Zhang C, Hu W, Feng Z. Tumor suppressor p53 and metabolism. *Journal of Molecular Cell Biology*. 2019;11(4):284-292. doi:10.1093/jmcb/mjy070
48. Lemberg KM, Gori SS, Tsukamoto T, Rais R, Slusher BS. Clinical development of metabolic inhibitors for oncology. *The Journal of Clinical Investigation*. 01/04/ 2022;132(1)doi:10.1172/JCI148550
49. Oatman N DN, Arora P, Choi K, Gawali MV, Gupta N, Parameswaran S, Salomone J, Reisz JA, Lawler S, Furnari F, Brennan C, Wu J, Sallans L, Gudelsky G, Desai P, Gebelein B, Weirauch MT, D'Alessandro A, Komurov K, Dasgupta B. Mechanisms of stearoyl CoA desaturase inhibitor sensitivity and acquired resistance in cancer *Science Advances*. 2021;7(7):eabd7459. doi:doi: 10.1126/sciadv.abd7459.

50. Vivas-García Y, Falletta P, Liebing J, et al. Lineage-Restricted Regulation of SCD and Fatty Acid Saturation by MITF Controls Melanoma Phenotypic Plasticity. *Molecular Cell*. 2020/01/02/ 2020;77(1):120-137.e9. doi:https://doi.org/10.1016/j.molcel.2019.10.014
51. Lien EC, Westermark AM, Zhang Y, et al. Low glycaemic diets alter lipid metabolism to influence tumour growth. *Nature*. 2021/11/01 2021;599(7884):302-307. doi:10.1038/s41586-021-04049-2
52. Lenoir WF, Morgado M, DeWeirdt PC, et al. Discovery of putative tumor suppressors from CRISPR screens reveals rewired lipid metabolism in acute myeloid leukemia cells. *Nature Communications*. 2021/11/11 2021;12(1):6506. doi:10.1038/s41467-021-26867-8
53. Metz HE, McGarry Houghton A. Insulin Receptor Substrate Regulation of Phosphoinositide 3-Kinase. *Clinical Cancer Research*. 2011;17(2):206-211. doi:10.1158/1078-0432.CCR-10-0434
54. Mauvoisin D, Mounier C. Hormonal and nutritional regulation of SCD1 gene expression. *Biochimie*. 2011/01/01/ 2011;93(1):78-86. doi:https://doi.org/10.1016/j.biochi.2010.08.001
55. Kiyatkin A, van Alderwerelt van Rosenburgh IK, Klein DE, Lemmon MA. Kinetics of receptor tyrosine kinase activation define ERK signaling dynamics. *Science Signaling*. 2020/08/18 2020;13(645):eaaz5267. doi:10.1126/scisignal.aaz5267
56. Kamphorst JJ, Cross JR, Fan J, et al. Hypoxic and Ras-transformed cells support growth by scavenging unsaturated fatty acids from lysophospholipids. *Proceedings of the National Academy of Sciences*. 2013/05/28 2013;110(22):8882-8887. doi:10.1073/pnas.1307237110
57. Casado P WE, Miraki-Moud F, Hadi MM, Rio-Machin A, Rajeeve V, Pike R, Iqbal S, Marfa S, Lea N, Best S, Gribben J, Fitzgibbon J, Cutillas PR. Proteomic and genomic integration identifies kinase and differentiation determinants of kinase inhibitor sensitivity in leukemia cells. *Leukemia*. 2018;32(8):1818-1822.
58. Rodencal J, Dixon SJ. A tale of two lipids: Lipid unsaturation commands ferroptosis sensitivity. https://doi.org/10.1002/pmic.202100308. *PROTEOMICS*. 2023/03/01 2023;23(6):2100308. doi:https://doi.org/10.1002/pmic.202100308
59. Magtanong L, Ko P-J, To M, et al. Exogenous Monounsaturated Fatty Acids Promote a Ferroptosis-Resistant Cell State. *Cell Chemical Biology*. 2019/03/21/ 2019;26(3):420-432.e9. doi:https://doi.org/10.1016/j.chembiol.2018.11.016
60. Eagle K, Jiang Y, Shi X, et al. An oncogenic enhancer encodes selective selenium dependency in AML. *Cell Stem Cell*. 2022/03/03/ 2022;29(3):386-399.e7. doi:https://doi.org/10.1016/j.stem.2022.01.003
61. Gallipoli P, Giotopoulos G, Tzelepis K, et al. Glutaminolysis is a metabolic dependency in FLT3ITD acute myeloid leukemia unmasked by FLT3 tyrosine kinase inhibition. *Blood*. 2018;131(15):1639-1653. doi:10.1182/blood-2017-12-820035
62. Woodley K, Dillingh LS, Giotopoulos G, et al. Mannose metabolism inhibition sensitizes acute myeloid leukaemia cells to therapy by driving ferroptotic cell death. *Nature Communications*. 2023/04/14 2023;14(1):2132. doi:10.1038/s41467-023-37652-0

FIGURE LEGENDS

Figure 1. SCD expression is prognostic in AML and SCD inhibition induces cell death in a subset of AML cell lines.

(A) Kaplan-Meier curves comparing overall survival and disease-free survival in TCGA AML patient cohort dichotomized after *SCD* expression. Expression level of *SCD* was considered a continuous variable and Log rank (Mantel-Cox) test was used for determining significance. (B) Forest plot of overall survival analyses considering continuous *SCD* gene expression on several patients' datasets. Multivariate analysis corrected for confounding variables like age, gender and ELN prognostic group in all datasets. (C) Single sample gene set enrichment analysis (ssGSEA) on TCGA cohort in dependency to *SCD* expression. (D) Gene set enrichment analysis (GSEA) for KEGG pathway Biosynthesis of unsaturated fatty acids and (E) TCGA-generated SCD signature in paired diagnosis-relapse primary AML samples (NEJM1808777 dataset). (F) Tumor burden and SCD signature expression in AraC-treated PDX models (GSE97631) and GSEA for SCD signature at MRD stage (E) A panel of eight AML cell lines was treated with SSI-4 (0.01 - 10 µM) or corresponding vehicle for 72h. Cells with less than 10% decrease in viability were designated resistant. Results are presented as non-linear regression of normalized response and data points are mean ± SEM. * $p < 0.05$, ** $p < 0.01$, *** $p < 0.001$, **** $p < 0.0001$.

Figure 2. SSI-4 sensitive cells display higher levels of SCD expression and enzymatic activity.

(A) Significantly enriched MSigDB signatures in sensitive vs resistant cell lines from Cancer Cell Line Encyclopedia proteomics dataset ranked by combined score from *Enrichr* enrichment analysis. Significantly upregulated signatures in sensitive cells are presented on the right hand-side and down-regulated signatures on the left hand-side of the graph. (B) Normalized expression of fatty acid synthesis related proteins in AML cell lines tested. (C) Representative western blot of sensitive (K562, MOLM-13, MV-4-11) and resistant (OCI-AML3, THP-1, HL-60) cell lines treated with SSI-4 (1 µM) or vehicle control for 24h. (D) Densitometric analysis shows SCD expression normalized to ß-actin as loading control. (E) MOLM-13, MV-4-11 and OCI-AML3 were treated with SSI-4 (1 µM) or vehicle control for 24h. Graph represents ratio of C16 and C18 saturated (SFA) and monounsaturated fatty acids (MUFA). (F) Schematic representation of *de novo* fatty acid synthesis pathway and SFA/MUFA imbalance upon SCD inhibition in sensitive and resistant cells. ACLY - ATP-citrate lyase, ACC1 – acetyl-CoA carboxylase, FASN – fatty acid synthase, ELOVL6 - ELOVL fatty acid elongase 6, SCD-1 – stearoyl-Co desaturase. (G) MOLM-13, MV-4-11 and OCI-AML3 were grown in medium supplemented with ^{13}C-Glucose (2 g/L) and treated with SSI-4 (1 µM) or vehicle control for 24h. Graphs represents percentage of ^{13}C-glucose incorporation in palmitate (C16:0), stearate (C18:0), palmitoleate (C16:1) and oleate (C18:1). Data are mean ± SEM. * $p < 0.05$, ** $p < 0.01$, *** $p < 0.001$, **** $p < 0.0001$.

Figure 3. SFA/MUFA ratio and lipotoxicity in response to SCD inhibition depend on the activity of FAS pathway.

(A, C) MOLM-13, MV-4-11 and OCI-AML3 were labelled with ^{13}C-Glucose (2 g/L) and treated for 24h with SSI-4 (1 µM) or vehicle control with or without the addition of oleate (100 µM) or palmitate (100 µM). Graphs represents percentage of ^{13}C-glucose incorporation in palmitate (C16:0) and oleate (C18:1) (B, D) MOLM-13, MV-4-11 and OCI-AML cells were treated for 72h with SSI-4 (1 µM) with or without addition of oleate (100 µM) or palmitate (100 µM). (E-G) Representative western blots of MOLM-13 cells treated for 24h with SSI-4 (1 µM) or vehicle control with or without addition of oleate (100 µM) or direct AMPK activator MK-8722 (10 µM). (H) MOLM-13 cells were treated for 72h with SSI-4 (1 µM) with or without addition of FASN inhibitor Fasnall (20 µM) or MK-8722 (10 µM). Viable

cells were determined as Annexin-V$^-$/PI$^-$. Data are mean ± SEM.* $p < 0.05$, ** $p < 0.01$, *** $p < 0.001$, **** $p < 0.0001$.

Figure 4. SSI-4 treatment induces both an increase in lipid peroxidation and activation of apoptotic machinery.

(A) Significantly enriched KEGG pathway signature in MV-4-11 cells treated with with SSI-4 (1 µM) or vehicle control for 24h. (B) Sensitive K562, MOLM-13, MV-4-11 and resistant OCI-AML3, THP-1, HL-60 and Kasumi-1 cell were treated for 24h with SSI-4 (1 µM) or vehicle control. Lipid peroxidation was measured using Bodipy C11. (C) Lipidomics analysis on MV-4-11 cells treated for 24h with SSI-4 (1 µM) or vehicle control. Upper graph represents enrichment analysis per lipid groups of SSI-4 treated cells in comparison to control (Q1-Q3 with line at median value) with significant lipid groups marked in red. Lower graph represents significant differentially expressed individual lipids with upregulated lipids presented on the right hand-side and down-regulated lipids on the left hand-side of the graph. Red bars: padj < 0.05. (D) MV-4-11 and MOLM-13 cells were treated for 72h with SSI-4 (1 µM) or vehicle control with or without addition of Ferrostatin-1 (5 µM). (E) MOLM-13 cells in early apoptosis (Annexin-V$^+$/PI$^-$) after 72h treatment with SSI-4 (1 µM). (F) Representative western blot of MOLM-13 and OCI-AML3 cells treated for 72h with SSI-4 (1 µM) or vehicle control with or without addition of oleate (100 µM) or palmitate (100 µM). (G) MOLM-13 and MV-4-11 cells were treated for 72h with SSI-4 (1 µM) or vehicle control with or without addition of Q-VD-OPh (50 µM). Viable cells were determined as Annexin-V$^-$/PI$^-$. Data are mean ± SEM. * $p < 0.05$, ** $p < 0.01$, *** $p < 0.001$, **** $p < 0.0001$.

Figure 5. SSI-4 has antileukemic effects on a subset of primary AML patient samples both *in vitro* and *in vivo* with sensitive samples showing higher levels of MUFA.

(A) AML primary samples (n=36) were depleted of T-cells and grown in co-culture with irradiated MS-5 cells for 7 days with addition of SSI-4 (1 µM). Samples with less than 5% decrease in viability were designated to resistant group. (B) Phosphorylated IRS2 in sensitive (n=5) vs resistant (n=11) samples measured using phosphoproteomic analyses. Graphs represent relative intensity of phosphopeptides. (C-D) MUFA levels and SFA/MUFA ratio in sensitive (n=4) vs resistant (n=7) samples. (E) Two sensitive (viability decrease > 20%) samples *in vitro* were transplanted into NBSGW mice. When engraftment of human CD45$^+$ cells exceeded 5% in the BM, animals were treated with 10 mg/kg of SSI-4 or corresponding vehicle orally for 14 days. Total number of human leukemic cells (hCD45$^+$hCD33$^+$hCD19$^-$) isolated from two legs at the end of the experiment. (F) In hCD45$^+$hCD33$^+$ cells isolated from mice transplanted with AML5 sample lipid peroxidation was measured using Bodipy C11. Viable cells were determined as Annexin-V$^-$/PI$^-$. Data are mean ± SEM. * $p < 0.05$, ** $p < 0.01$, *** $p < 0.001$, **** $p < 0.0001$.

Figure 6. SSI-4 demonstrates no hematopoietic toxicity but, as single agent, does not prolong survival in a mouse AML model.

(A) C57BL/6 mice (n=15) were treated with 10 and 30 mg/kg SSI-4 or corresponding vehicle orally for a total of 21 days with 2 days break after each 5 days of continuous treatment. PB counts of control or SSI-4 treated mice. WBC – white blood cells, RBC – red blood cells, HGB – haemoglobin concentration, HCT – haematocrit, MCV – mean cell volume, MCH – mean cell haemoglobin, MCHC – mean cell haemoglobin concentration, PLT – platelets. (B) Gating strategy and total numbers of cells in LSK (Lin$^-$Sca-1$^+$c-Kit$^+$), HPC-1 (LSK CD48$^+$CD150$^-$), HPC-2 (LSK CD48$^+$CD150$^-$), HSC (LSK CD48$^-$CD150$^+$), MPP (LSK CD48$^-$CD150$^-$) compartments in the BM isolated from two legs of treated animals. (C) Leukemic *Hoxa9/Meis1* and *iMLL-AF9* cells were treated with SSI-4 (0.01-10 µM)) or corresponding

vehicle (DMSO). (D) Leukemic *Hoxa9/Meis1* and *iMLL-AF9* cells were treated with SSI-4 (1 µM) or vehicle control with or without addition of oleate (100 µM) for 48h. (E) CD45.2$^+$ LSK (Lin$^-$Sca-1$^+$c-Kit$^+$) cells from *iMLL-AF9* mice were transplanted to lethally irradiated syngeneic CD45.1$^+$/CD45.2$^+$ recipient mice (n=10). After engraftment was confirmed in PB, animals were treated with 10 mg/kg SSI-4 or corresponding vehicle orally for 20 days. Percentage of CD45.2$^+$/Mac-1$^+$/Gr-1$^+$ and CD45.2$^+$/Mac-1$^+$/Gr-1$^-$ cells in the BM at the end of the experiment. (F) In CD45.2$^+$ cells lipid peroxidation was measured using Bodipy C11. (G) Murine AML model was established as described in (E). After engraftment was confirmed in PB, animals (n=14) were treated with 10 mg/kg SSI-4 or corresponding vehicle *orally* for a total of 21 days with 2 days break after each 5 days of continuous treatment. Percentage of CD45.2$^+$/Mac-1$^+$/Gr-1$^+$ and CD45.2$^+$/Mac-1$^+$/Gr-1$^-$ cells in PB at the end of treatment with SSI-4. (H) Kaplan-Meier curve comparing overall survival of animals treated with SSI-4 and corresponding vehicle (control). Viable cells were determined as Annexin-V$^-$/PI$^-$ or Annexin-V$^-$/7-AAD$^-$. Data are mean ± SEM. * $p < 0.05$, ** $p < 0.01$, *** $p < 0.001$, **** $p < 0.0001$.

Figure 7. Lipotoxicity increases DNA damage and SSI-4 acts synergistically with DNA damage inducing chemotherapy both *in vitro* and *in vivo*.

(A-B) Representative western blots of MV-4-11 cells treated with SSI-4 (1 µM) or vehicle control with or without addition of oleate (100 µM), palmitate (100 µM) or doxorubicin (1 µM) for 24h. (C) MV-4-11 NT gRNA, SCD gRNA 1 and SCD gRNA 2 were treated for 72h with doxorubicin (1 µM). (D) MV-4-11 and leukemic iMLL-AF9 cells were treated for 72h with growing concentrations of SSI-4 and doxorubicin. Synergy was determined by Bliss coefficient (ZIP Score > 10 indicates synergism). (E) MV-4-11 cells were transplanted into NBSGW mice (n=28). 14 days after transplant animals were treated for 9 days with 10 mg/kg SSI-4 or corresponding vehicle *orally* with or without receiving conventional chemotherapy protocol (3 days 1.0 mg/kg doxorubicin i.v., 5 days 50 mg/kg cytarabine i.v.). Kaplan-Meier curve comparing overall survival of animals treated with SSI-4 and corresponding vehicle with our without conventional chemotherapy. (F) CD45.2$^+$ leukemic *iMLL-AF9* cells were transplanted into CD45.1$^+$ NBSGW mice (n=18). When leukemic burden in PB reached 20%, animals were treated for 7 days with 10 mg/kg SSI-4 or corresponding vehicle *orally* with or without receiving conventional chemotherapy protocol (3 days 1.0 mg/kg doxorubicin i.v., 5 days 50 mg/kg cytarabine i.v.). Kaplan-Meier curve comparing overall survival of animals treated with SSI-4 and corresponding vehicle with our without conventional chemotherapy. Viable cells were determined as Annexin-V$^-$/PI$^-$ or Annexin-V$^-$/Zombie$^-$. Data are mean ± SEM. * $p < 0.05$, ** $p < 0.01$, *** $p < 0.001$, **** $p < 0.0001$.

Figure 1

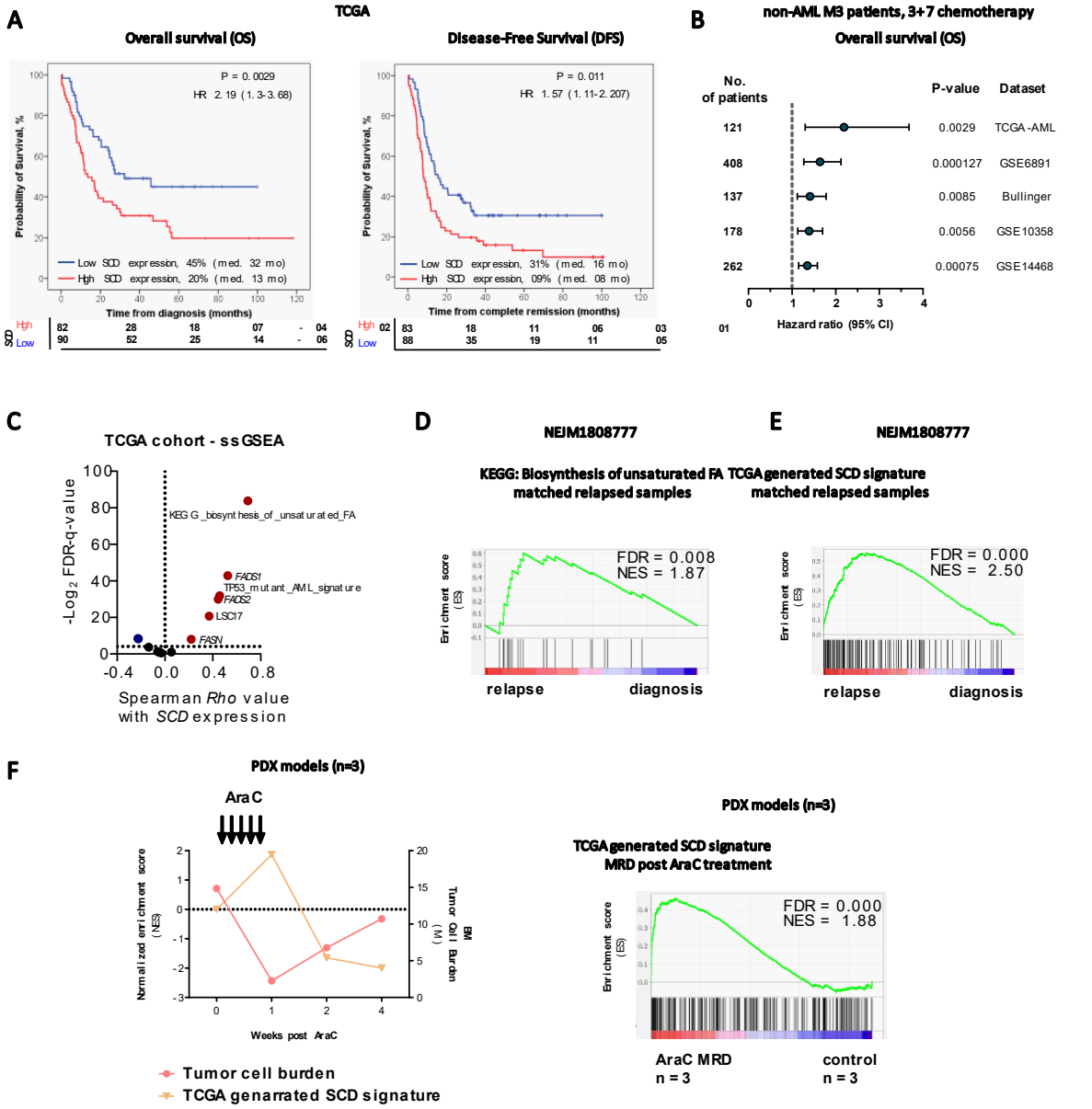
A
TCGA
Overall survival (OS)
Disease-Free Survival (DFS)
P = 0.0029
HR 2.19 (1.3-3.68)
P = 0.011
HR 1.57 (1.11-2.207)
Probability of Survival, %
Low SCD expression, 45% (med. 32 mo)
High SCD expression, 20% (med. 13 mo)
Low SCD expression, 31% (med. 16 mo)
High SCD expression, 09% (med. 08 mo)
Time from diagnosis (months)
Time from complete remission (months)
B
non-AML M3 patients, 3+7 chemotherapy
Overall survival (OS)
No. of patients
P-value
Dataset
121 0.0029 TCGA-AML
408 0.000127 GSE6891
137 0.0085 Bullinger
178 0.0056 GSE10358
262 0.00075 GSE14468
Hazard ratio (95% CI)
C
TCGA cohort - ssGSEA
-Log2 FDR-q-value
KEGG_biosynthesis_of_unsaturated_FA
FADS1
TP53_mutant_AML_signature
FADS2
LSC17
FASN
Spearman Rho value with SCD expression
D
NEJM1808777
KEGG: Biosynthesis of unsaturated FA matched relapsed samples
FDR = 0.008
NES = 1.87
Enrichment score (ES)
relapse
diagnosis
E
NEJM1808777
TCGA generated SCD signature matched relapsed samples
FDR = 0.000
NES = 2.50
F
PDX models (n=3)
AraC
Normalized enrichment score (NES)
Tumor Cell Burden (%) BM
Weeks post AraC
Tumor cell burden
TCGA genarrated SCD signature
PDX models (n=3)
TCGA generated SCD signature MRD post AraC treatment
FDR = 0.000
NES = 1.88
AraC MRD n = 3
control n = 3
G
SSI-4
relative viability (%)
K562 (IC50 = 40 nM)
MOLM-13 (IC50 = 47 nM)
MV-4-11 (IC50 = 11 µM)
log[10] concentration (M)
SSI-4
OCI-AML3 (IC50 = 234.5 µM)
THP-1 (IC50 = 211.4 µM)
HL-60 (IC50 = 79.4 µM)
Kasumi-1 (IC50 = 116.8 µM)
TF-1 (IC50 = 191.5 µM)

Figure 2

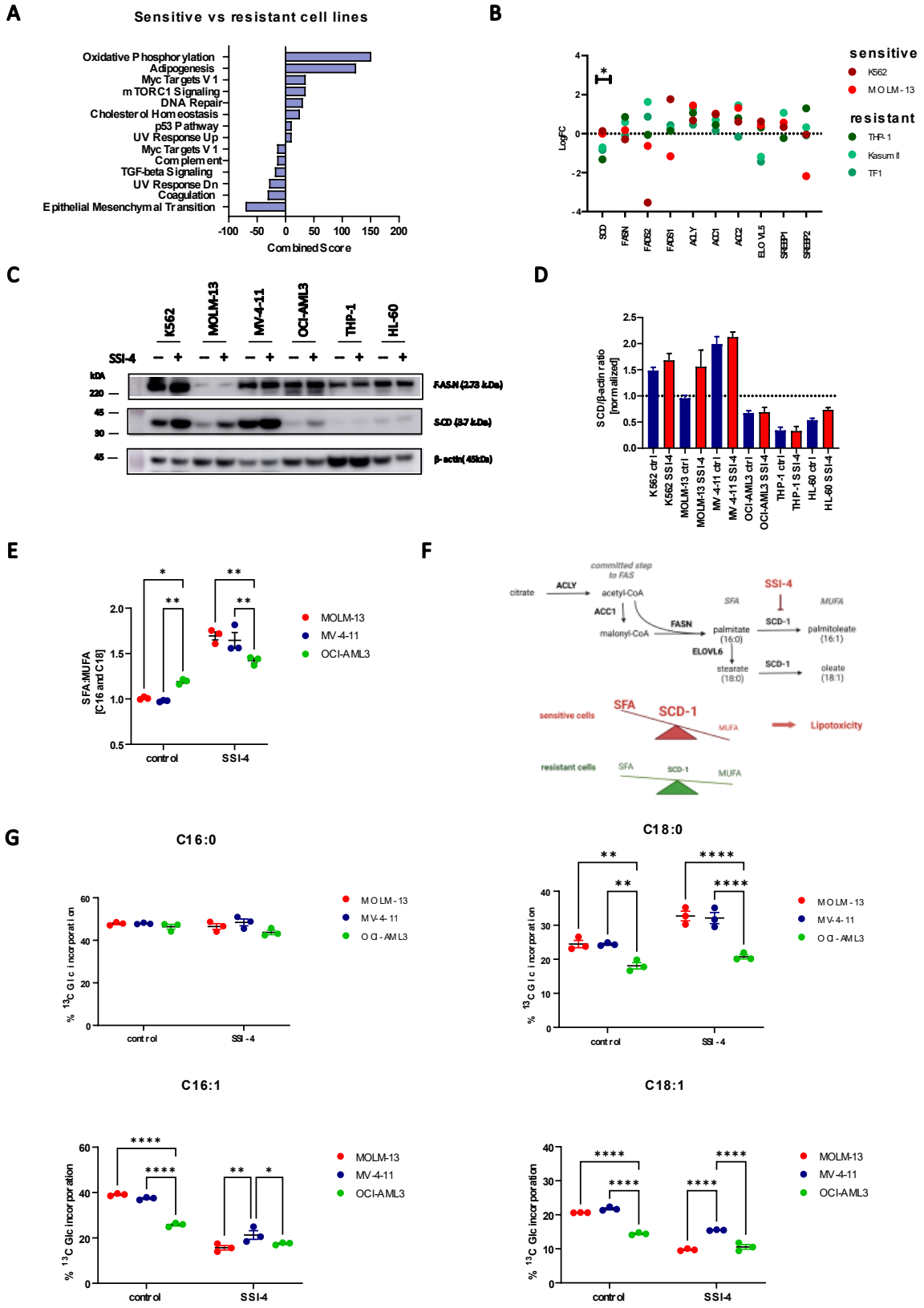
A
Sensitive vs resistant cell lines
Oxidative Phosphorylation
Adipogenesis
Myc Targets V1
mTORC1 Signaling
DNA Repair
Cholesterol Homeostasis
p53 Pathway
UV Response Up
Myc Targets V1
Complement
TGF-beta Signaling
UV Response Dn
Coagulation
Epithelial Mesenchymal Transition
Combined Score
B
sensitive
K562
MOLM-13
resistant
THP-1
Kasumi II
TF1
LogFC
SCD
FASN
FADS2
FADS1
ACLY
ACC1
ACC2
ELOVL5
SREBP1
SREBP2
C
K562
MOLM-13
MV-4-11
OCI-AML3
THP-1
HL-60
SSI-4
kDA
FASN (273 kDa)
SCD (37 kDa)
β-actin (45kDa)
D
SCD/β-actin ratio [normalized]
K562 ctrl
K562 SSI-4
MOLM-13 ctrl
MOLM-13 SSI-4
MV-4-11 ctrl
MV-4-11 SSI-4
OCI-AML3 ctrl
OCI-AML3 SSI-4
THP-1 ctrl
THP-1 SSI-4
HL-60 ctrl
HL-60 SSI-4
E
SFA:MUFA [C16 and C18]
control
SSI-4
MOLM-13
MV-4-11
OCI-AML3
F
committed step to FAS
citrate
ACLY
acetyl-CoA
ACC1
malonyl-CoA
FASN
palmitate (16:0)
ELOVL6
stearate (18:0)
SSI-4
SFA
MUFA
SCD-1
palmitoleate (16:1)
oleate (18:1)
sensitive cells
resistant cells
Lipotoxicity
G
C16:0
C18:0
C16:1
C18:1
% 13C Glc incorporation
control
SSI-4
MOLM-13
MV-4-11
OCI-AML3

Figure 3

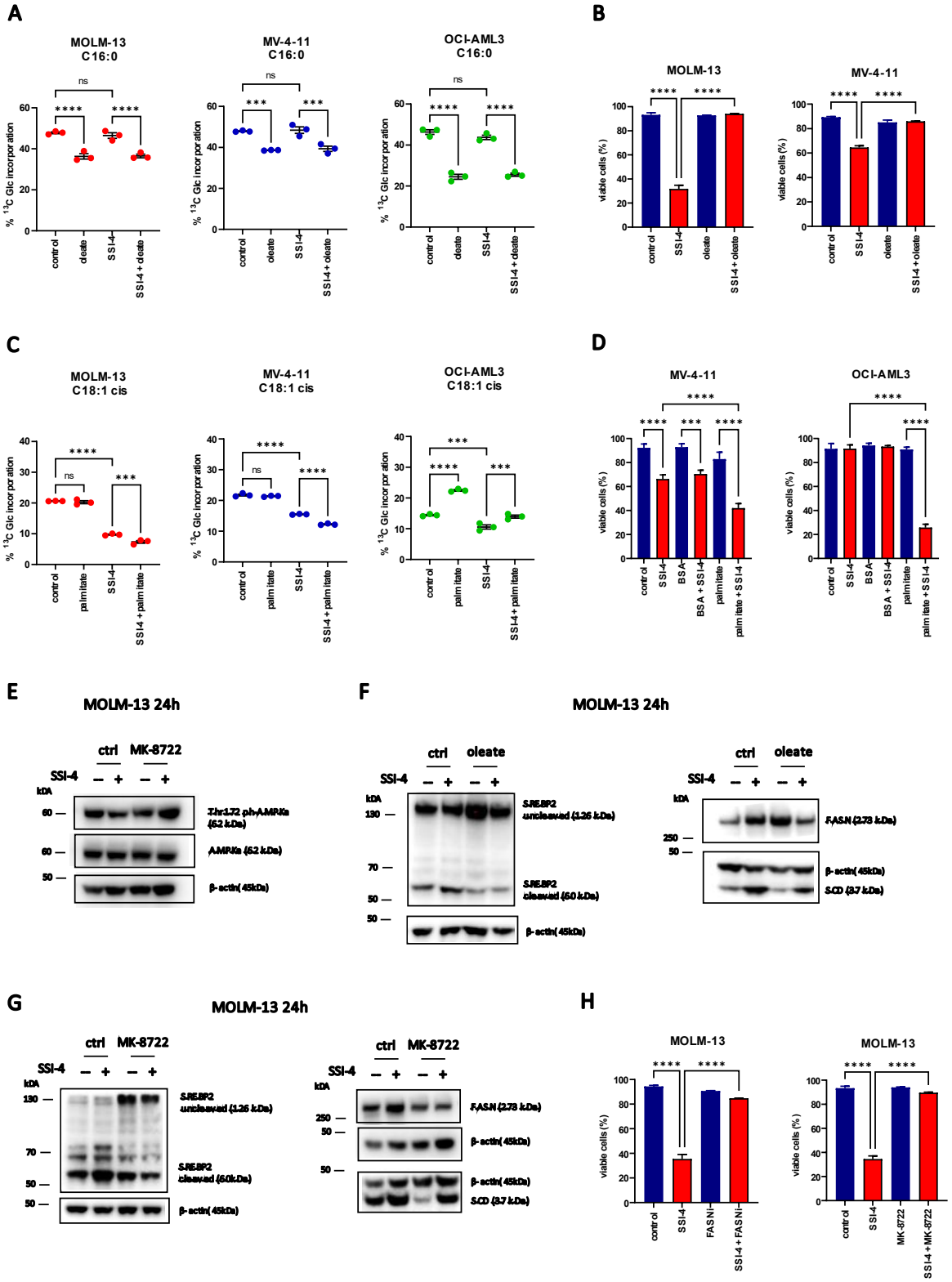
A
MOLM-13
C16:0
MV-4-11
C16:0
OCI-AML3
C16:0
% 13C Glc incorporation
control
oleate
SSI-4
SSI-4 + oleate
B
MOLM-13
MV-4-11
viable cells (%)
C
MOLM-13
C18:1 cis
MV-4-11
C18:1 cis
OCI-AML3
C18:1 cis
palmitate
SSI-4 + palmitate
D
MV-4-11
OCI-AML3
BSA
BSA + SSI-4
palmitate + SSI-4
E
MOLM-13 24h
ctrl
MK-8722
SSI-4
kDA
Thr172 ph-AMPKa (62 kDa)
AMPKa (62 kDa)
β-actin(45kDa)
F
MOLM-13 24h
ctrl
oleate
SREBP2 uncleaved (126 kDa)
SREBP2 cleaved (60 kDa)
FASN (273 kDa)
SCD (37 kDa)
G
MOLM-13 24h
H
MOLM-13
FASNi
SSI-4 + FASNi
SSI-4 + MK-8722

Figure 4

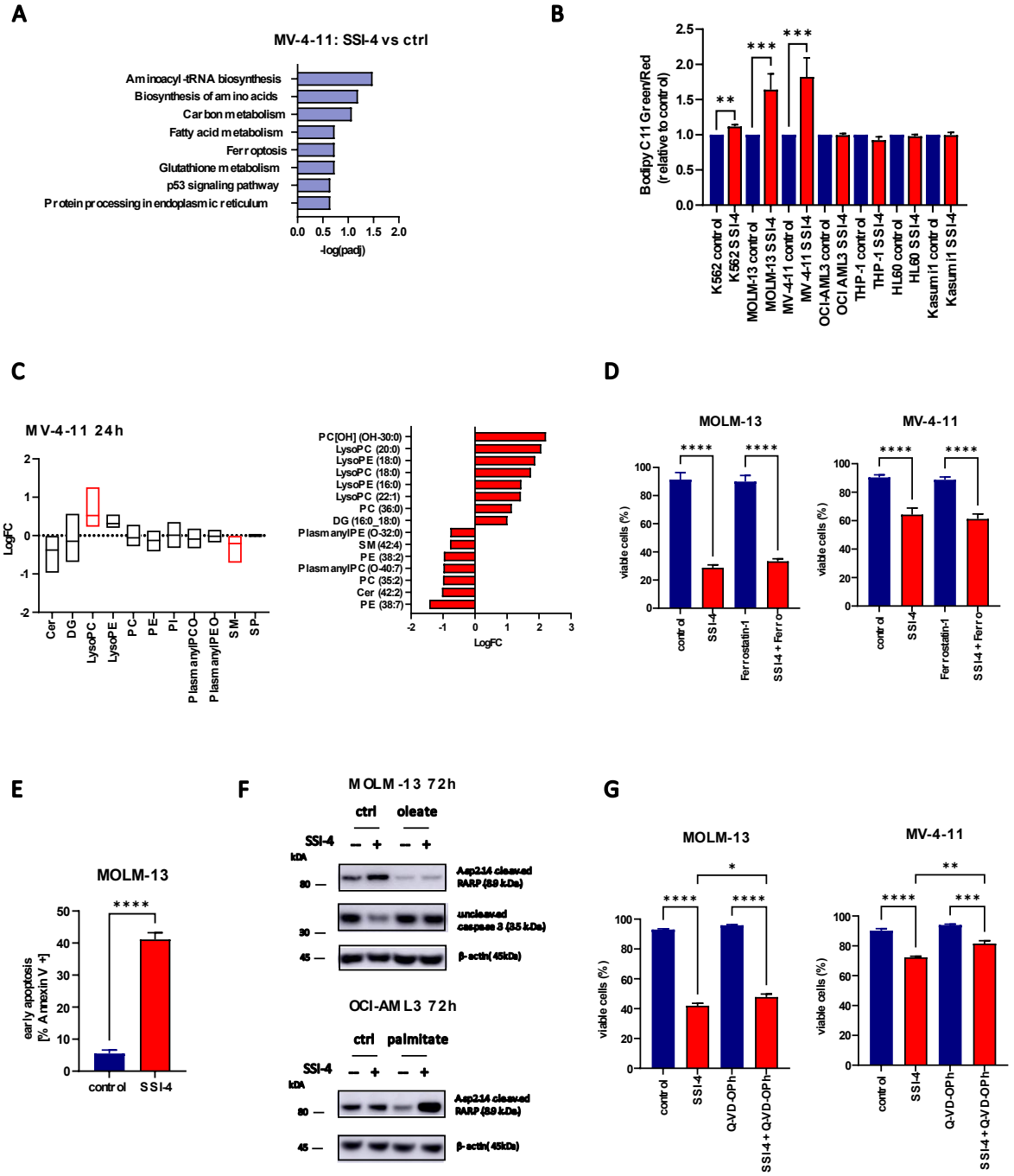
A
MV-4-11: SSI-4 vs ctrl
Aminoacyl-tRNA biosynthesis
Biosynthesis of amino acids
Carbon metabolism
Fatty acid metabolism
Ferroptosis
Glutathione metabolism
p53 signaling pathway
Protein processing in endoplasmic reticulum
-log(padj)
B
Bodipy C11 Green/Red (relative to control)
K562 control
K562 SSI-4
MOLM-13 control
MOLM-13 SSI-4
MV-4-11 control
MV-4-11 SSI-4
OCI-AML3 control
OCI AML3 SSI-4
THP-1 control
THP-1 SSI-4
HL60 control
HL60 SSI-4
Kasumi1 control
Kasumi1 SSI-4
C
MV-4-11 24h
LogFC
Cer
DG
LysoPC
LysoPE
PC
PE
PI
PlasmanylPCO
PlasmanylPEO
SM
SP
PC[OH] (OH-30:0)
LysoPC (20:0)
LysoPE (18:0)
LysoPC (18:0)
LysoPE (16:0)
LysoPC (22:1)
PC (36:0)
DG (16:0_18:0)
PlasmanylPE (O-32:0)
SM (42:4)
PE (38:2)
PlasmanylPC (O-40:7)
PC (35:2)
Cer (42:2)
PE (38:7)
D
MOLM-13
MV-4-11
viable cells (%)
control
SSI-4
Ferrostatin-1
SSI-4 + Ferro
E
MOLM-13
early apoptosis [% Annexin V +]
control
SSI-4
F
MOLM-13 72h
ctrl
oleate
SSI-4
kDA
Asp214 cleaved RARP (89 kDa)
uncleaved caspase 3 (35 kDa)
β-actin (45kDa)
OCI-AML3 72h
ctrl
palmitate
SSI-4
kDA
Asp214 cleaved RARP (89 kDa)
β-actin (45kDa)
G
MOLM-13
MV-4-11
viable cells (%)
control
SSI-4
Q-VD-OPh
SSI-4 + Q-VD-OPh

Figure 5

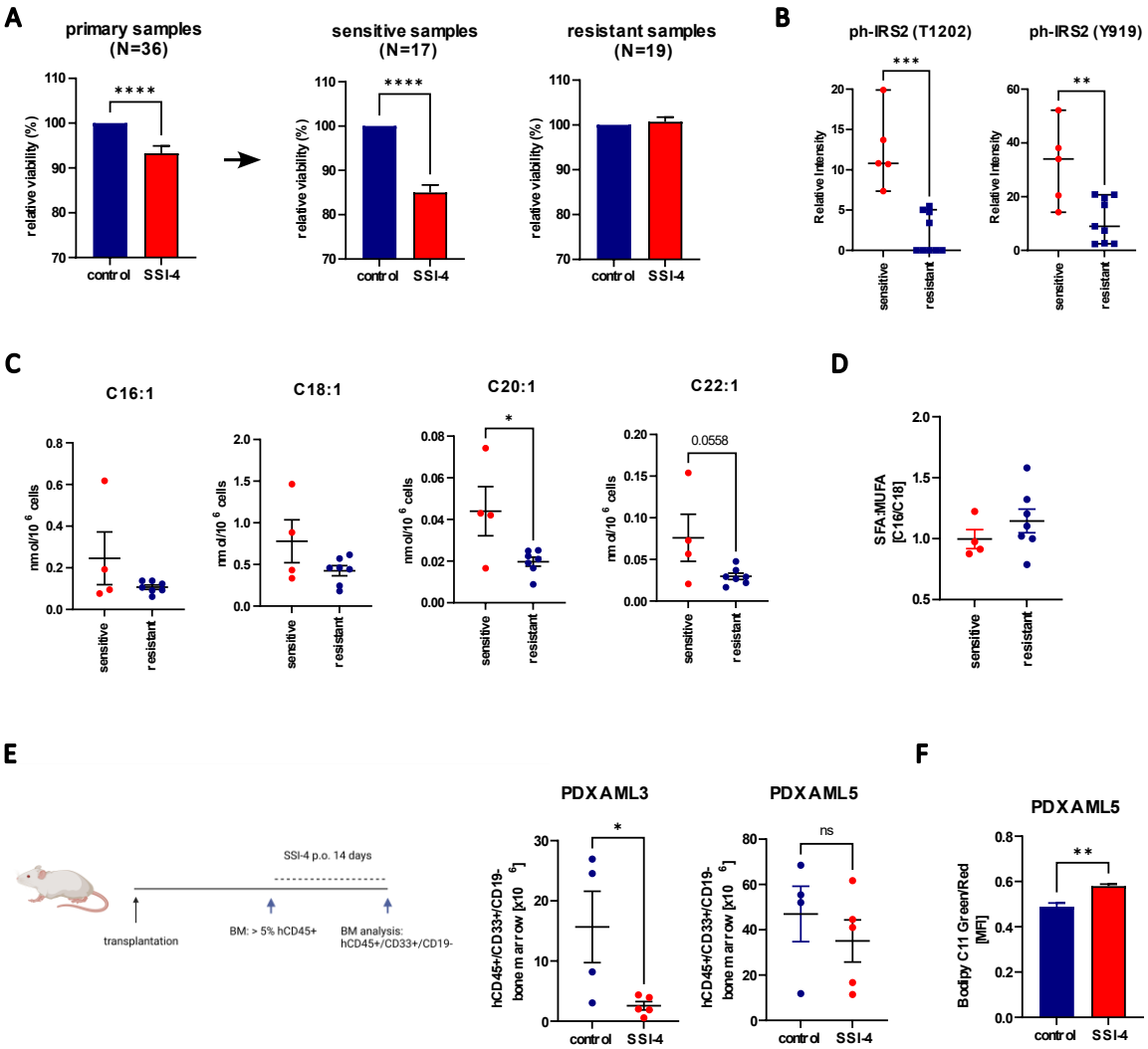
A
primary samples (N=36)
sensitive samples (N=17)
resistant samples (N=19)
relative viability (%)
control
SSI-4
****
B
ph-IRS2 (T1202)
ph-IRS2 (Y919)
Relative Intensity
sensitive
resistant
***
**
C
C16:1
C18:1
C20:1
C22:1
nmol/10 6 cells
*
0.0558
D
SFA/MUFA [C16/C18]
E
SSI-4 p.o. 14 days
transplantation
BM: > 5% hCD45+
BM analysis: hCD45+/CD33+/CD19-
PDXAML3
PDXAML5
hCD45+/CD33+/CD19- bone marrow [x10 6]
ns
F
Bodipy C11 Green/Red [MFI]
**

Figure 6

A

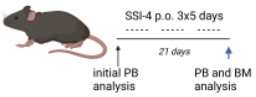

	control	SSI-4 10 mg/kg	SSI-4 30 mg/kg
	mean ± SEM	*mean ± SEM*	*mean ± SEM*
WBC [10^3/µL]	10.46 ± 0.49	10.2 ± 2.43	9.34 ± 0.29
RBC [10^6/µL]	11.32 ± 0.29	10.34 ± 1.43	10.7 ± 0.24
HGB [g/dL]	15.2 ± 0.25	13.52 ± 1.95	14.5 ± 0.31
HCT [%]	50.64 ± 0.85	45.46 ± 6.20	48.4 ± 0.88
MCV [fL]	44.8 ± 0.55	44.04 ± 0.41	45.22 ± 0.41
MCH [pg]	13.44 ± 0.14	13.04 ± 0.16	13.54 ± 0.13
MCHC [g/dL]	30.02 ± 0.10	29.52 ± 0.49	29.94 ± 0.11
PLT [10^3/µL]	575 ± 27	483 ± 79	562 ± 34

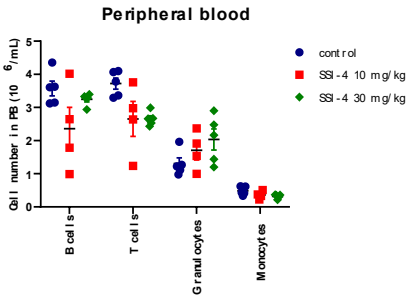

B

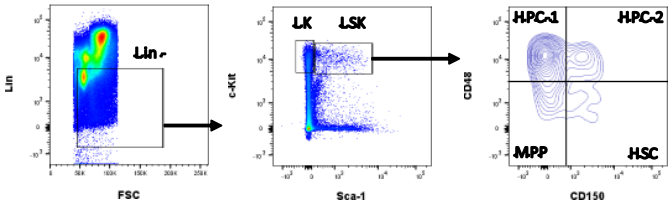

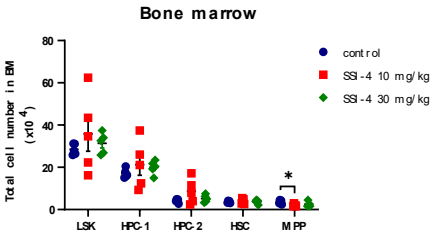

C

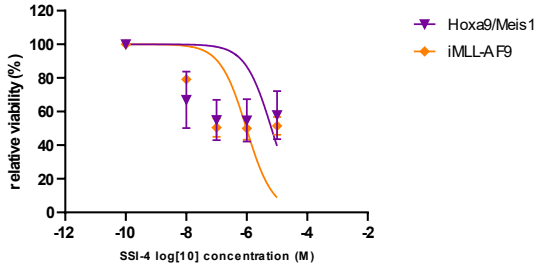

D

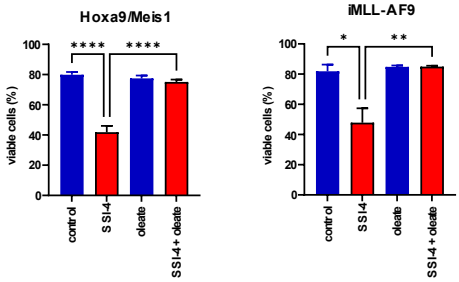

E

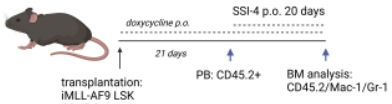

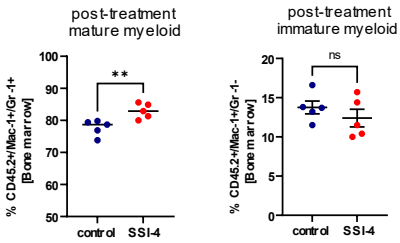

F

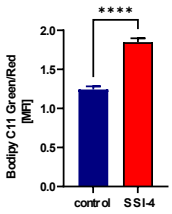

G

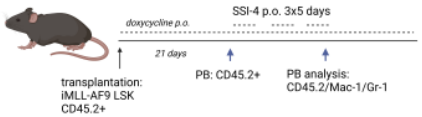

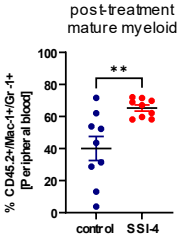

H

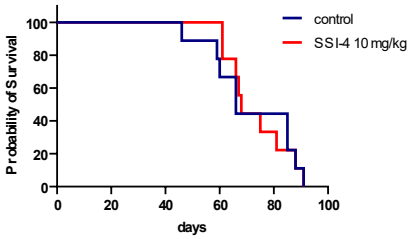

Figure 7

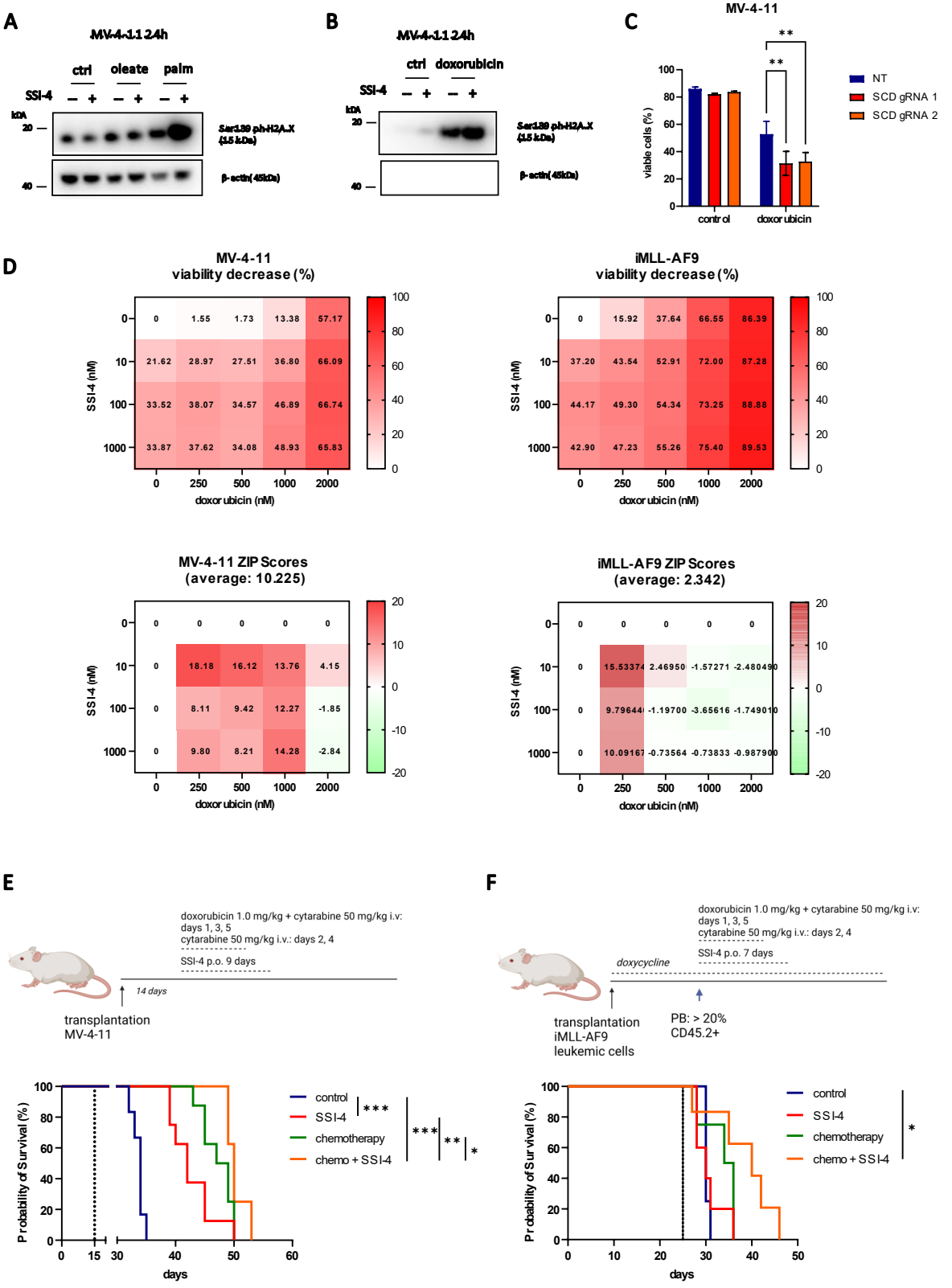
A
MV-4-11 24h
ctrl
oleate
palm
SSI-4
kDA
20
40
Ser139 ph-H2A.X (15 kDa)
β-actin (45kDa)
B
MV-4-11 24h
ctrl
doxorubicin
SSI-4
kDA
20
40
Ser139 ph-H2A.X (15 kDa)
β-actin (45kDa)
C
MV-4-11
viable cells (%)
control
doxorubicin
NT
SCD gRNA 1
SCD gRNA 2
D
MV-4-11 viability decrease (%)
iMLL-AF9 viability decrease (%)
SSI-4 (nM)
doxorubicin (nM)
MV-4-11 ZIP Scores (average: 10.225)
iMLL-AF9 ZIP Scores (average: 2.342)
E
doxorubicin 1.0 mg/kg + cytarabine 50 mg/kg i.v: days 1, 3, 5
cytarabine 50 mg/kg i.v.: days 2, 4
SSI-4 p.o. 9 days
14 days
transplantation MV-4-11
Probability of Survival (%)
days
control
SSI-4
chemotherapy
chemo + SSI-4
F
doxorubicin 1.0 mg/kg + cytarabine 50 mg/kg i.v: days 1, 3, 5
cytarabine 50 mg/kg i.v.: days 2, 4
SSI-4 p.o. 7 days
doxycycline
transplantation iMLL-AF9 leukemic cells
PB: > 20% CD45.2+
Probability of Survival (%)
days
control
SSI-4
chemotherapy
chemo + SSI-4